

Evolution of granitic magmas during ascent: A phase equilibrium model

MARTHA L. SYKES

Department of Geology, Arizona State University, Tempe, AZ 85287, U.S.A.*

and

JOHN R. HOLLOWAY

Departments of Chemistry and Geology, Arizona State University, Tempe, AZ 85287, U.S.A.

Abstract—Evolution of granitic magma during ascent through the crust is modelled by using phase relationships and thermodynamic properties of the system albite–H₂O, by assuming fluid-absent conditions. Pressure–temperature ascent trajectories are calculated for particular crystallization rates and H₂O contents using an expression for the albite liquidus temperature as a function of pressure and H₂O activity. Increased H₂O content causes a decrease in initial temperature of trajectories, and a decrease in dP/dT for a crystallization rate (CR) of 10% per kbar and an increase in dP/dT for all melting rates (MR). The H₂O activity in the magma continuously increases during ascent for MR < 4% per kbar and all CR's. Ascent trajectories for all CR's and MR's < about 2% have positive dP/dT . Adiabatic ascent trajectories have positive but steep dP/dT and require fusion of pre-existing (restitute) crystals when present. These results suggest that restite-bearing magmas commonly undergo continued melting (resorption) during ascent, thus avoiding superheating even for nearly adiabatic ascent trajectories.

Thermodynamic and physical properties of the magma system are calculated along ascent trajectories. Volume increases during ascent for CR ≤ 5 to 6% per kbar and, at high H₂O contents, is more strongly a function of crystallization rate than H₂O content; change in volume may exceed 10% overall. The enthalpy change is exothermic during ascent provided MR < 7% per kbar; internal energy change during ascent is exothermic for MR ≤ 3% per kbar. Magma (melt + crystal) density is nearly constant along ascent trajectories, whereas melt density decreases during ascent. For intermediate to high H₂O contents, magma and melt viscosities are about constant along ascent trajectories for CR > 0% per kbar. At low total H₂O contents and CR = 10% per kbar, magma viscosity increases by up to four orders of magnitude; melt viscosity remains nearly constant. Energy available from an ascending granitic magma body as calculated from enthalpy and internal energy changes can reach two to three times the values calculated by using heat capacity data; this necessitates reconsideration of certain magma transport processes.

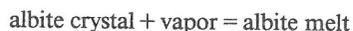
INTRODUCTION

THE "GRANITE CONTROVERSY" of the first part of this century (READ, 1957; WALTON, 1955) has been largely resolved: most researchers agree that granitic¹ rocks crystallize from parental melts formed by partial fusion of source rocks in the upper mantle or crust. Since CHAPPELL and WHITE (1974) championed the concept that granitic magmas inherit the characteristics of their source regions, great progress has been made in understanding chemical and mineralogical variations among suites of granitic rocks. However, the mechanisms for transport of granitic magmas between source and emplacement level, and the processes that occur during such transport, remain largely unstudied and unconstrained. For example, restite segregation has been

proposed as a geochemically viable process occurring between source and emplacement level, but its physical feasibility has not been demonstrated.

To address such problems, thermodynamics and phase equilibria of the system albite–H₂O are used to model the evolution of granitic magma during transport from source towards the surface. For given crystallization or melting rates, calculated pressure–temperature trajectories for a constant mass of magma allow evaluation of variations in magma properties (*e.g.*, volume, density, enthalpy, entropy, internal energy, viscosity) during ascent. Implications for processes important during transport of granitic magmas are presented in this paper.

Few theoretical studies of granitic magma evolution during ascent exist. Isentropic adiabats valid for multiphase, multicomponent systems calculated for albite–H₂O by RUMBLE (1976), show that adiabatic decompression along the univariant curve defined by the reaction



* Now at Texas Wesleyan College, Department of Physics/Geology, Fort Worth, Texas 76105-9989.

¹ The terms "granitic" and "granite" here signify any calc-alkaline intrusive rock of composition from tonalite to granite, *sensu stricto*.

results in crystallization, whereas adiabatic decompression through the crystal + melt field results in melting. WALDBAUM (1971) calculated isenthalpic temperature rise during decompressive ascent of magmas by using Joule-Thompson coefficients, but neglected the change in gravity potential of the vertically moving masses, which invalidates his conclusions (RAMBERG, 1971).

Fluid dynamic studies of magma transport have been largely restricted to mantle conditions. Reviews by SPERA (1980) and TURCOTTE (1982) serve to emphasize the lack of quantitative descriptions of crustal magma transport. Diapiric transport of andesitic magma from the upper mantle through the crust has been evaluated using heat transfer models (MARSH, 1978; MARSH and KANTHA, 1978; MARSH, 1982), and fluid dynamic models. Elastic crack propagation, proposed as a major mechanism for basaltic magma transport (*e.g.*, SHAW, 1980; see also TURCOTTE, 1987), has not been directly applied to granitic rocks. Stopping can be a major transport mechanism for magmas only near the earth's surface (MARSH, 1982).

Models for granitic magma transport must explain differences between deep and shallow emplacement of granitic magma, and any inherent differences in the physical, chemical, or mineralogical properties of such magma systems.

Symbols used in thermodynamic and phase equilibrium calculations are as given in Table 1, unless otherwise defined in the text.

THE MODEL

Evolution of granitic magma during ascent is modelled using phase relationships for the system albite-H₂O (BURNHAM and DAVIS, 1971, 1974; BURNHAM, 1979). Model granitic magma consists of albite melt, dissolved H₂O, and variable amounts of albite crystals. Pressure-temperature ascent trajectories are calculated for a specified crystallization or melting rate (denoted CR and MR, respectively; given as weight percent crystals formed or melted per kbar of ascent) and volatile content by using a relationship for albite liquidus temperature as a function of *P* and H₂O activity (*a_w*).

Specification of a particular crystallization or melting rate defines the amount of heat and energy transfer from the system, once an ascent mechanism and body size and shape are defined. Certain of the ascent trajectories may therefore be considered unlikely due to excessively slow velocities required for heat transfer during crystallization, or because they require input of energy for some MR > 0%/kbar paths. Variations of enthalpy and internal energy

Table 1. Symbols and abbreviations used.

<i>a</i>	—activity of component
ab	—albite
<i>C_p</i>	—heat capacity, J/g-K
CR	—crystallization rate, in weight percent per kbar
<i>E</i>	—internal energy, J/g
<i>G</i>	—free energy, J/g
<i>g</i>	—constant of gravitational acceleration, 980 cm/s ²
<i>H</i>	—enthalpy, J/g
<i>K</i>	—thermal diffusivity, cm/s ²
<i>k</i>	—Henry's law constant
<i>m</i>	—mass of system, g
MR	—melting rate, in weight percent per kbar
<i>n</i>	—mole
<i>P</i>	—pressure, kbar
<i>q</i>	—heat energy
<i>r</i>	—radius, cm
<i>R</i>	—gas constant, 8.314 J/mol-K
<i>S</i>	—entropy, J/g-K
<i>T</i>	—temperature, K
<i>V</i>	—volume, cm ³
<i>v</i>	—velocity, cm/s
<i>W</i>	—weight fraction
<i>w</i>	—work energy
<i>X</i>	—mole fraction
<i>z</i>	—vertical coordinate
Δ	—difference between two quantities
μ	—viscosity, poise
ρ	—density, g/cm ³
φ	—volume fraction
β	—adiabatic gradient, K/km
α	—coefficient of thermal expansion, K ⁻¹
Pe	—Peclet number, vr/K

Superscripts and subscripts

w	—H ₂ O
xl	—crystal
o	—initial condition or standard state
wr	—wall rock
s	—solid
m	—melt
fl	—fluid
fus	—fusion
gl	—glass

for the magma system during ascent, given in a later section, reflect these heat transfer requirements. If a model for heat transfer is assumed, the enthalpy or internal energy data can be incorporated, allowing limitations to be made on ascent velocity and body size (or shape) for a particular trajectory (SYKES, 1986).

Constant values of CR and MR were chosen for ease of calculation. Ascent trajectories for nonlinear rates can be interpolated between those calculated.

Assumptions

In the present model for granitic magma ascent, the system albite-H₂O is used as an analogue for

hydrous granitic magma. Solubility relationships of H₂O in albite melt adequately represent those for most granitic magmas (quartz- or hypersthene-normative, calc-alkaline composition), provided that melt compositions are expressed in an eight-oxygen albite-equivalent form (BURNHAM, 1979). Volume and thermodynamic properties of hydrous albite melt are also applicable to granitic magmas (BURNHAM and DAVIS, 1974); values for these properties are most accurate in the range 1 to 10 kbar.

Liquidus curves at constant X_w^m for the system albite-H₂O have similar slopes, dT/dP , to those for actual granitic magmas. For albite-H₂O, dT/dP decreases with both increasing pressure and X_w^m . This relationship also holds for crystalline phases of fixed composition in granitic magmas; the magnitude of the decrease in dT/dP depends on $S_{gl} - S_{sl}$, such that the smaller the difference, ΔS , the greater the decrease in dT/dP (BURNHAM and DAVIS, 1974).

Absolute temperatures of liquidus and solidus curves are greater for albite-H₂O than for actual granitic magmas. However, this temperature discrepancy has little effect on H₂O solubilities. BURNHAM (1979) notes that equimolar solubilities for the Harding pegmatite are duplicated by albite-H₂O within experimental error ($X_w^m \pm 0.02$) despite a 450°C difference in temperature. It will be shown in the following section that the higher temperatures for albite-H₂O have similarly small effect on ascent trajectories.

The major limitations of using albite-H₂O as a granite analogue are that the role of changing composition during differentiation, and the effects of hydrous phase crystallization (or melting), cannot be rigorously evaluated. The former limitation can be addressed by incorporation of BURNHAM's (1981) activity-composition relationships for multicomponent aluminosilicate melts into the liquidus temperature calculations. Such an approach is not used in the present model because details of phase equilibria effects, although of importance in considering evolution of particular granitic magmas, tend to obscure the effects of H₂O and simple crystal-melt equilibria on ascent trajectories and physical properties of the magmas (see also NEKVASIL and BURNHAM, 1987). The effect of hydrous phase crystallization on X_w^m and ascent trajectories depends on the rate of crystallization during ascent, as will be shown after discussion of ascent trajectory calculation.

In these model calculations, H₂O is assumed to be the dominant volatile component. Abundant evidence for the presence of H₂O exists, including the presence of hydrous phases such as micas and

amphiboles, and experimentally determined phase relationships for particular granitic rocks. Evidence for the presence of volatile species relatively insoluble in silicic melts, such as CO₂, and the existence of a separate fluid phase in the early stages of granitic magmatism, is generally lacking.

Calculated values for physical and thermodynamic properties represent spatial averages for a particular batch of magma; *i.e.*, a homogeneous distribution of crystals and volatiles is assumed. Any vertical extent of the magma body is ignored: no external pressure gradients are assumed to exist over the magma body. Ascending magma is considered to be closed with respect to addition or loss of aluminosilicate material. The major processes assumed to be affecting the magma are crystallization, melting, and dissolution of H₂O.

A major assumption of the model is that of chemical equilibrium in the ascending batch of magma. This assumption requires that processes occurring during magma ascent be reversible. For closed magma systems this assumption is good: irreversible physical processes such as viscous dissipation are insignificant compared to reversible energy sources and sinks, such as crystallization, melting and volatile exsolution. Irreversible heat and momentum transfer processes are excluded from the present model for granitic magma ascent and evolution; their effects will be considered in later papers.

Calculation of albite liquidus temperature

Albite liquidus temperature is calculated as a function of pressure and X_w^m with the relationship:

$$\ln(a_{ab}^m/a_{ab}^s) = -\frac{\Delta G_{ab}^{m0} + (P-1)\Delta V_{ab}^m}{RT}, \quad (1)$$

where a_{ab}^m and a_{ab}^s are the activities of anhydrous albite in the melt (m) and solid (s) phases, respectively, relative to $a_{ab}^m = 1$ in melt of pure albite, and $a_{ab}^s = 1$ in pure albite solid (BURNHAM, 1979). P is pressure in bar, T is in K, and ΔV_{ab}^m is the volume of melting of pure albite. The quantity $\Delta G_{ab}^{m0} + (P-1)\Delta V_{ab}^m$ can be expressed as a function of pressure and temperature. This allows an explicit equation for albite liquidus temperature for $X_w^m \leq 0.5$:

$$T = \frac{b}{R\{0.58 - \ln[(1 - X_w^m)^2]\} - c}, \quad (2)$$

and for $X_w^m > 0.5$:

$$T = \frac{(b/R) - 2667[\ln(1 - X_w^m) + X_w^m] - 515}{0.707 - (c/R) - 6.52[\ln(1 - X_w^m) + X_w^m]}, \quad (3)$$

where $b = 229.2P + 1.3075 \times 10^4$; $c = -2.0597 \times 10^{-3}P^2 - 6.6918 \times 10^{-3}P - 8.3172$; R is in cal/mol-K, T in K, and P in kbar. Parameters b and c derive from fitting the quantity $\Delta G + P\Delta V$ as a function of pressure and temperature. The quantity 0.58 in Equation (2) is an empirical correction factor required for differences in tabulated free energy data used in BURNHAM's (1979) and the current analysis of Equation (1). Activity relationships for H_2O in albite melt are taken from BURNHAM (1979; his equations 16-3 and 16-4), with $a_w^m = a_w^f = 1$ at H_2O saturation. For $X_w^m \leq 0.5$:

$$a_w = k(X_w^m)^2, \quad (4)$$

and for $X_w^m > 0.5$:

$$a_w = 0.25k \exp(6.52 - 2667/T)(X_w^m - 0.5), \quad (5)$$

where T is in K, and k is a Henry's law activity constant analogue, and a function of pressure, and to a lesser extent temperature. Activity relationships for the albite component in hydrous melt are given by BURNHAM (1979; his Equations 16-13 and 16-14). Calculated liquidus temperatures agree closely with those of BURNHAM (1979) and BOETTCHER *et al.* (1982).

Calculation of ascent paths

The general method of calculating ascent trajectories using the model system albite- H_2O discussed by HOLLOWAY (1976) has been modified to include the calculation of the liquidus temperature of albite given in Equations (2) and (3) and additional model parameters. The sequence of calculation follows:

(1) Specify initial pressure, H_2O content (weight percent), and initial and final crystal content (this determines CR or MR).

(2) Calculate initial $X_w^m = n_w/(n_w + n_{\text{ab}}^m)$.

(3) Albite liquidus temperature is calculated as a function of pressure and X_w^m .

(4) Pressure is decreased by a small amount, P , and the calculation repeated. The ΔP must be small enough so that $dP/dT \approx \Delta P/\Delta T$. Convergence of dP/dT and $\Delta P/\Delta T$ is almost reached at $\Delta P = 0.005$ kbar, but the differences in calculated values are less than the uncertainty in thermodynamic values, thus a ΔP of 0.01 kbar is used. The calculation is stopped when the H_2O -saturated solidus of the system has been reached: the system completely crystallizes and evolves a fluid phase.

Typical ascent trajectories for different crystallization rates are shown in Figure 1. The shape and position of the ascent path is independent of initial crystal content for equivalent CR's. In standard

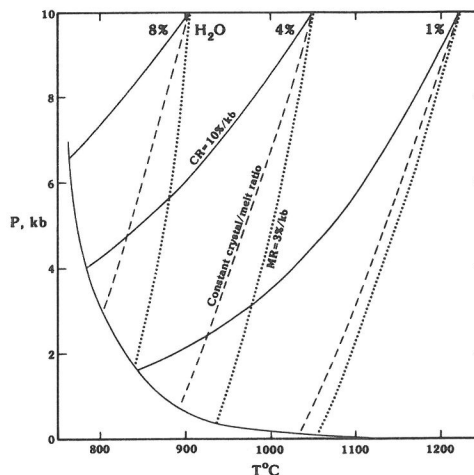


FIG. 1. Typical ascent trajectories calculated using the present model, for 1, 4, and 8 weight percent H_2O in the system. Solid lines represent a crystallization rate of 10%/kbar ($\text{CR} = 10\%/kbar$) dashed lines represent a constant crystal/melt ratio and dotted lines represent a melting rate of 3%/kbar ($\text{MR} = 3\%/kbar$). The light solid line that terminates ascent trajectories is the H_2O -saturated solidus for albite.

phase diagrams for albite- H_2O , the field to the right of the $\text{CR} = 0\%/kbar$ trajectory (liquidus isopleth) would consist only of melt at high pressures, and become melt + fluid at some lower pressure. Ascent trajectories for $\text{MR} > 0\%/kbar$ apparently cross the melt + fluid region. However, for $\text{MR} > 0\%/kbar$, crystals are defined as being initially present in the magma, so the field is actually crystal + melt, the amount of melt being limited by the H_2O available. As pressure decreases during ascent and melting of these initially present crystals proceeds, X_w^m decreases, so that the melt + fluid (or melt + crystal + fluid) field is never reached.

All trajectories shown have positive dP/dT , including those for fusion of pre-existing crystals during ascent. Trajectory slope is positive for $\text{MR}'s < 3$ to 4%/kbar for 1 to 8 weight percent H_2O in the melt.

The H_2O content affects both shape and position of ascent trajectories. Increased total H_2O content causes the initial temperature to decrease by 30 to 60°C per weight percent H_2O added to the system in the range 1 to 8 weight percent H_2O for a given initial pressure. Increased total H_2O content causes a decrease in dP/dT for $\text{CR} > 0\%/kbar$ and an increase in dP/dT for $\text{MR} \geq 0\%/kbar$, as expected from the albite- H_2O model. $\text{CR} = 0\%/kbar$ curves correspond to liquidus isopleths.

The most important characteristic for comparing ascent trajectories of model and actual granitic sys-

tems is trajectory shape. Ascent trajectories for higher CR's allow greater discrimination among possible volatile contents due to their more eccentric shapes. A decrease in initial pressure has no effect on trajectory shape: the CR = 0%/kbar trajectory remains the same, and the CR = 10%/kbar trajectory is lowered.

Trajectory shape depends largely on X_w^m , which in turn is a function of temperature. Because liquidus temperatures for albite-H₂O are greater by up to several hundred degrees than liquidus temperatures for actual granitic compositions, the effect of temperature on X_w^m and trajectory shape was tested. In the present model, the effect of temperature on X_w^m is governed by the Henry's law constant, k , used in Equations (4) and (5). Temperature dependence of k is greatest at low pressure. Test calculations were made by calculating k at 200°C lower than trajectory temperature with 1 and 8 weight percent H₂O. The X_w^m was increased by 1 and 5% at 10 kbar and 1 kbar, respectively. Ascent trajectories shift to temperatures lower by less than 3°C.

Crystallization of hydrous phases is not part of the albite-H₂O model system. The effect of hydrous phase crystallization on X_w^m can, however, be estimated by computing the amount of H₂O that would be removed from the melt by crystallizing a particular amount of the hydrous phase. For example, crystallization of 200 g of hornblende or biotite would remove about 4 or 8 g of H₂O from the system. The effect on ascent trajectory shape depends

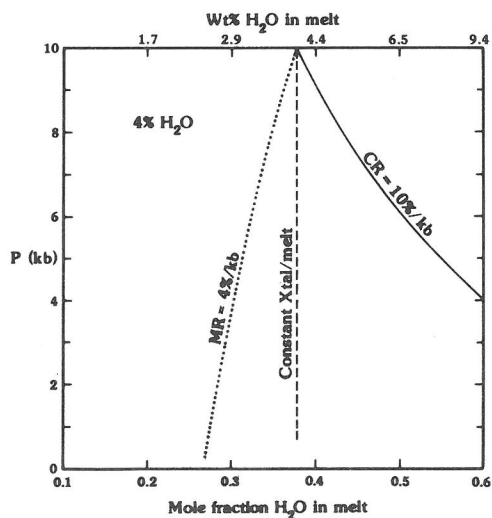


FIG. 2. Variation along ascent trajectories in X_w^m (and weight percent H₂O in melt) for 4 weight percent H₂O in the system at various crystallization rates. Curves designated as in Figure 1.

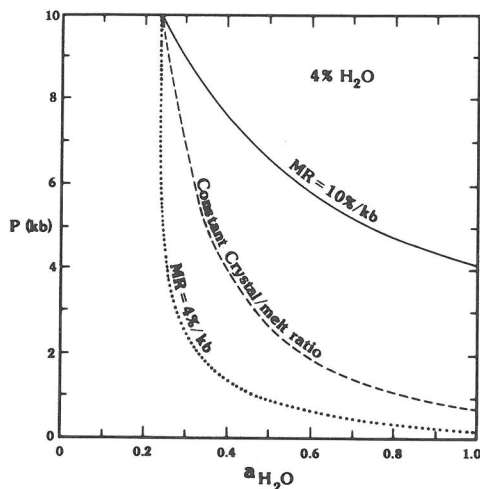


FIG. 3. Variation in activity of H₂O (a_w) along ascent trajectories for 4 weight percent H₂O in the system at various crystallization rates. Curves designated as in Figure 1. Note that the intersection of a curve with $a_{H_2O} = 1$ signifies that the H₂O-saturated solidus has been reached, and no liquid can exist at lower pressure.

on the crystallization rate for the hydrous phase and H₂O content of the system. For 1 weight percent H₂O in the system, crystallization of 20 weight percent hydrous phase at a single pressure would reduce X_w^m by about 75%, causing a shift in ascent trajectory to a higher temperature. For 8 weight percent H₂O in the magma, crystallization of 20% magma at a single pressure along the CR = 0%/kbar trajectory causes a 6% increase in X_w^m ; the decrease in moles of melt due to crystallization has a greater effect on X_w^m than loss of H₂O to the hydrous phase. Crystallization of a hydrous phase at CR = 5%/kbar over the entire ascent distance results in ascent trajectories higher by only 1 to 2°C than those crystallizing anhydrous phases.

The change in proportions of phases along ascent trajectories reflected by X_w^m (Figure 2) also affects a_w (Figure 3). The H₂O activity in the magma continuously increases during ascent for all CR's, and for MR < 4%/kbar.

VARIATION IN MAGMA PROPERTIES DURING ASCENT

Using the pressure-temperature-composition data generated by the ascent trajectory calculations, any thermodynamic or physical property of magma that is a function of P , T , X_w or a_w can be evaluated. Partial molar thermodynamic properties for H₂O and ab components of the melt and ab crystal are calculated from equations given in BURNHAM and DAVIS (1974), by using relationships of the type:

$$F_{\text{magma}} = n_m F_m + n_{xl} F_{xl}$$

$$= (n_{ab}^m + n_w^m)(X_{ab}^m F_{ab}^m + X_w^m F_w^m) + n_{xl} F_{xl},$$

where F is any extensive thermodynamic property. Properties involving the component H_2O are calculated with a standard state based on the triple point of H_2O , necessitated by use of thermodynamic relationships from BURNHAM and DAVIS (1974).

Volume

Variation in volume, given as percent change from initial volume ($\Delta V/V_0$) is shown in Figure 4 as a function of volatile content for various crystallization rates. Important points to note for volume variation include:

(1) For a given volatile content, $\Delta V/V_0$ varies more strongly as a function of CR than pressure. Increase in total V_w^m for the system with increasing X_w^m compensates for volume decrease during crystallization. In general there will be some CR that results in a zero volume change for a given initial H_2O content. This zero volume change occurs at about CR = 6%/kbar for 1 weight percent H_2O and about CR = 5%/kbar for 8 weight percent H_2O .

(2) Volume increases do not exceed 10% from initial (10 kbar) values to final total pressures as low as 1 kbar even for H_2O -rich systems.

Enthalpy

Change in magma enthalpy for the system during ascent (ΔH), calculated as the difference in H between successive pressure-temperature-composition points, is shown in Figure 5 as a function of crystallization rate for 4 weight percent H_2O in the

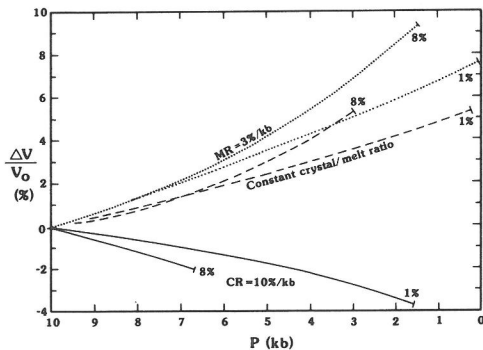


FIG. 4. Change in system volume from initial value at 10 kbar along ascent trajectories as a function of H_2O content and crystallization rate. Curves designated as in Figure 1. The figures in percent indicate system H_2O content. The intersection with the solidus is indicated by a bar perpendicular to the curves.

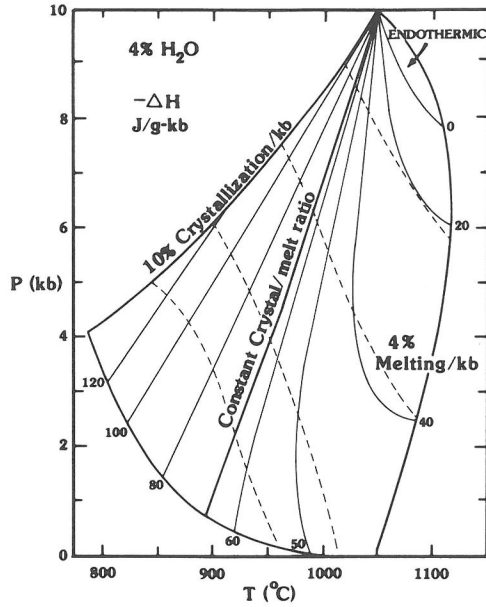


FIG. 5. Change in magma enthalpy along ascent trajectories for 4 weight percent H_2O in the system as a function of crystallization rate. Heavy solid lines are ascent trajectories as labelled. Light solid lines are contours of ΔH . Dashed lines are adiabats as discussed in the text.

system. ΔH is dependent on the ascent path, and approximately constant along any particular trajectory, ranging from about -120 to -70 J/g-kb, from 10 to 0%/kbar CR. The ΔH is usually exothermic and becomes endothermic only at MR $> 7\%$ /kbar.

Variations in ΔH as a function of volatile content and crystallization rate are shown in Figure 6. The ΔH becomes more exothermic with increased volatile content at CR = 10%/kbar; the reverse is true for CR = 0%/kbar. ΔH varies from -50 to -90 J/g-kb for CR = 10%/kbar and from about -20 to -35 J/g-kb for CR = 0%/kbar in the range 1 to 8 weight percent H_2O .

Typical isenthalpic adiabatic paths defined by

$$dH = -mgdz, \tag{6}$$

where m is mass, g is acceleration due to gravity, and z is a vertical coordinate, are shown by the dashed lines in Figure 5. For a particular depth interval $mgdz$ is constant; thus an infinite number of parallel adiabats exist. For all H_2O contents, isenthalpic adiabats require melting of crystals during ascent when crystals are initially present.

Entropy

Variation in S along ascent trajectories for 4 weight percent H_2O in the system is shown in Figure

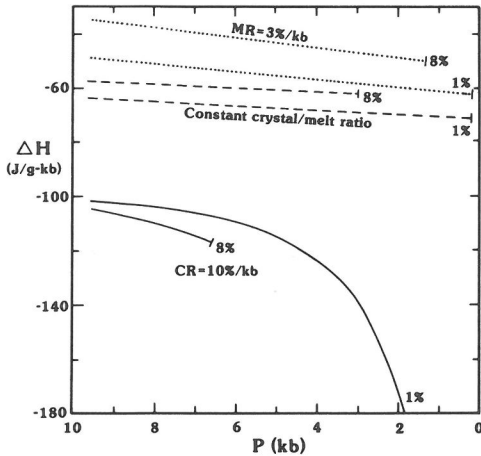


FIG. 6. Change in magma enthalpy along ascent trajectories as a function of crystallization rate and total H₂O content. Curves designated as in Figure 1. The figures in percent indicate system H₂O content. The intersection with the solidus is indicated by a bar perpendicular to the curve.

7. The S increases by about 0.3 J/g-K over the 10 kbar of ascent. The ΔS along ascent trajectories (not shown) is very small, usually less than -0.1 J/g-K-kbar . The constant entropy contours of Figure 7 define isentropic adiabats ($dS/dP = 0$) for that system. These differ from isenthalpic adiabats by

the amount $mgdz$ given in Equation (6). As for isenthalpic adiabats, melting of crystals, when present, must occur during isentropic adiabatic ascent.

Heat capacity

Heat capacities at constant pressure (C_p) for melt and magma are nearly constant. For all tested H₂O contents (0 to 8 weight percent) and crystallization rates (0 to 10%), the C_p varies only from about 1.38 to 1.51 J/g-K for the melt, and from about 1.26 to 1.46 J/g-K for magma. CR = 0%/kbar trajectories exhibit less variation in C_p than do paths with higher crystallization rates.

Internal energy

The change in internal energy, ΔE , along ascent trajectories is calculated by:

$$\Delta E = \Delta H - \Delta(PV). \quad (7)$$

Variation in ΔE during ascent is shown as a function of crystallization rate for 4 weight percent H₂O in the system (Figure 8); again ΔE is path dependent. Trends in ΔE are similar to those for ΔH , but ΔE is less exothermic due to the contribution of $\Delta(PV)$. The effect of volatile and crystal contents on ΔE are shown in Figure 9. ΔE is exothermic

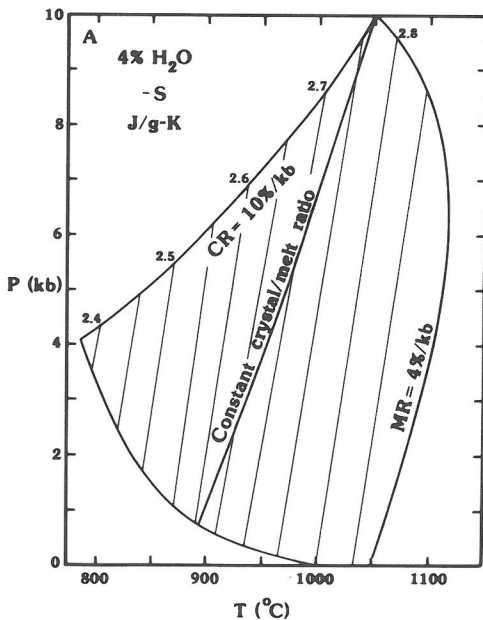


FIG. 7. Variation of entropy along ascent trajectories for 4 weight percent H₂O in the system. Heavy solid lines are ascent trajectories as labelled. Light solid lines are contours of entropy, which are also adiabats for the system.

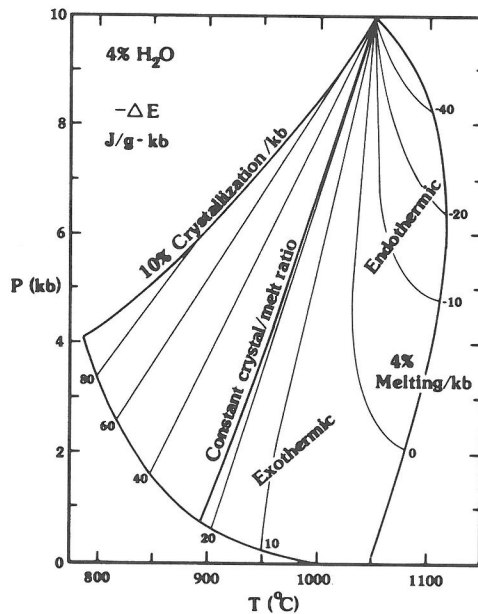


FIG. 8. Change in magma internal energy along ascent trajectories for 4 weight percent H₂O in the system as a function of crystallization rate. Heavy solid lines are ascent trajectories as labelled. Light solid lines are contours of constant ΔE .

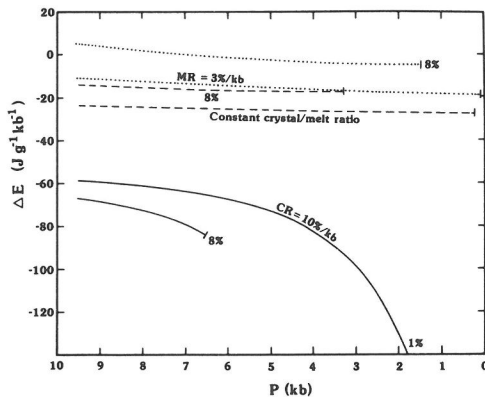


FIG. 9. Change in magma internal energy along ascent trajectories as a function of total magma H₂O content and crystallization rate. Curves designated as in Figure 1. The figures in percent indicate system H₂O content. The intersection with the solidus is indicated by a bar perpendicular to the curve.

for all CR's and for MR ≤ 3%/kbar for 4 weight percent H₂O in the system. As for Δ*H*, Δ*E* becomes increasingly exothermic with increasing H₂O contents at CR = 10%/kbar; the reverse is true for CR = 0%/kbar.

Density

Density of individual phases is calculated as the inverse of specific volume; magma density is calculated as:

$$\frac{1}{\rho_{\text{magma}}} = \frac{W_m}{\rho_m} + \frac{W_{xl}}{\rho_{xl}} + \frac{W_{fl}}{\rho_{fl}}, \quad (8)$$

where *W* is weight fraction of the phase. The absolute values of density may be lower than the densities of actual granitic compositions because mafic phases are excluded from the model. Magnitude and direction of variation of magma and melt density with temperature, pressure and H₂O content calculated in the present model should accurately reflect the competing effects of decompression, temperature decreases, crystallization, and melting for actual granitic magmas.

Density variation is expressed as ρ/ρ_0 , and is shown as a function of crystallization rate and volatile content in Figure 10 for melt and magma density. The ρ_{magma} is nearly constant along CR's, whereas ρ_m decreases during ascent. Near-constant ρ_{magma} is due to the compensating effects of crystallization and increasing X_w^m . An increase in total H₂O content of 1 weight percent results in a decrease in density of about 1% relative (*i.e.*, about 0.02 g/cm³ absolute).

Viscosity

Melt viscosity can be calculated as a function of *T* and X_w^m by using SHAW's (1972) empirical method, provided that an actual granitic magma composition is used. The melt composition used (Table 2) is the assumed initial (high pressure) composition of the Strathbogie granitoids (CLEMENS, 1981). The anhydrous melt composition is held constant; only the proportion of H₂O varies, thus "crystals" have the same composition as the melt. The resulting variations in melt viscosity, therefore, reflect only the effects of varying X_w^m . Pressure is assumed to have no effect on viscosity (but see also DINGWELL, 1987).

Albite liquidus temperatures are higher than those experimentally determined for granitic rocks, which would result in low melt viscosity values. Ascent trajectory temperatures are therefore arbitrarily reduced by 150°C for viscosity calculations.

The viscosity of magma (melt + crystal) is calculated by using the relationship:

$$\frac{\mu_{\text{magma}}}{\mu_m} = \left(1 - \frac{\pi}{4\alpha^2}\right) + \left(\frac{\pi}{4} - \frac{\pi}{6\alpha}\right) \left(\frac{1}{\alpha^2 - 1}\right) \times \left(1 + \frac{2}{\sqrt{\alpha^2 - 1}} \tan^{-1} \sqrt{\frac{\alpha + 1}{\alpha - 1}}\right), \quad (9)$$

(ACKERMANN and SHEN, 1979) where $\alpha = (\phi_\infty/\phi)^{1/3}$, and ϕ is volume fraction of crystals in the magma. ϕ_∞ is taken as 0.675, a value intermediate to the range of critical ϕ values found by VAN DER MOLEN and PATERSON (1979) to separate granular-flow from suspension-like behavior in partially melted granitic rocks. The maximum allowed μ_{magma} is 10¹⁵ poise, based on viscosity data for rhyolite summarized in SPERA *et al.* (1982). Calculated magma viscosity approximates non-Newtonian behavior in that the magma attains an effective yield strength (μ_{magma} goes to infinity) once the volume fraction of crystals in the magma reaches ϕ_∞ (0.675 in our calculation).

Viscosity as a function of CR and volatile content is shown in Figure 11 for melt and magma. For a given pressure, both μ_{magma} and μ_m increase with decreasing CR, equivalent to increasing temperature. The effect of increasing X_w^m is greater than increasing the amount of crystals on viscosity for these systems.

During ascent, μ_m increases slightly then decreases for CR = 10%/kbar; the approximation that μ_m is constant during ascent is good. For CR < 0%/kbar, μ_m increases, by up to two orders of magnitude. Magma viscosity always increases during ascent, initially by a factor of about 0.1 per kbar.

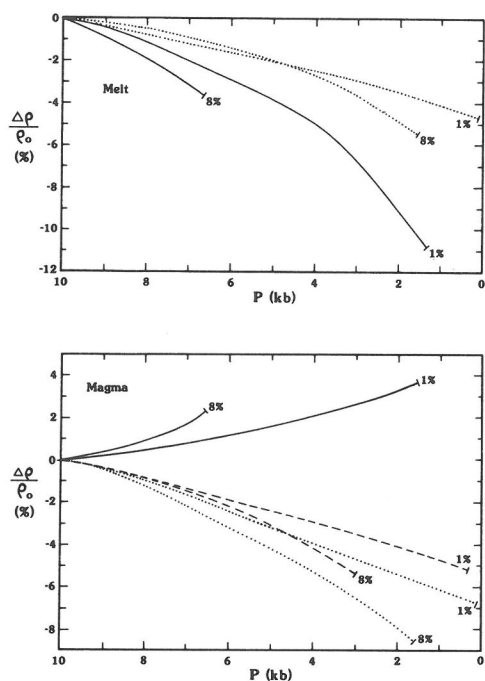


FIG. 10. Variation in density along ascent trajectories as a function of crystallization rate and H₂O content normalized to initial (10 kbar) density value. (a) Melt density. (b) Magma (crystal + melt) density. Curves designated as in Figure 1. The figures in percent indicate system H₂O content. The intersection with the solidus is indicated by a bar perpendicular to the curve.

Magma viscosity may increase by greater than three orders of magnitude over initial values for CR = 10%/kbar trajectories.

The presence of initial crystals results in an increase of the overall viscosity of the magma, and buffers changes in magma viscosity brought about by crystallization and changing X_w^m .

MODEL VALIDITY: THE STRATHBOGIE BATHOLITH AND VIOLET TOWN VOLCANICS

The major obstacle in the test of the present model for ascent trajectories and variation in magma properties is the paucity of experimental and physical data for actual granitic rocks: source region pressure and temperature, initial melt and magma composition, and amount of crystallization or fusion during ascent are adequately constrained for very few granitic rocks. Two of the best case histories found so far by the authors are for the Strathbogie batholith and Violet Town Volcanics of southeastern Australia (CLEMENS, 1981; CLEMENS and WALL, 1981, 1984). A combination of experimental, geochemical, and petrographic tech-

niques were used by CLEMENS (1981), together with field relationships, to provide tight constraints for initial (source) and final (emplacement) conditions for these "granitic" rocks.

The Strathbogie batholith

This late Devonian composite batholith discordantly intrudes folded Siluro-Devonian sedimentary rocks and cogenetic volcanic rocks. The batholith is subdivided into four mappable units based on grain size and composition. The Strathbogie granitoids are peraluminous S-types, generally containing cordierite, garnet and biotite in addition to plagioclase, quartz and K-feldspar. The most mafic variant of the Strathbogie batholith, a porphyritic microgranite (CLEMENS' sample number 889) contains 50 volume percent coarse phenocrysts; this composition is thought to represent that of initially emplaced magma (CLEMENS, 1981). Initial, ascent, and emplacement conditions deduced for the Strathbogie batholith by CLEMENS and WALL (1981) are given in Table 3. Based on H₂O content and sequence of crystallization, ascent trajectories for the Strathbogie magma are constrained to lie on the low temperature side of the quartz

Table 2. Compositions for Violet Town Volcanics and Strathbogie Granite (CLEMENS and WALL, 1984; CLEMENS, 1981)

Sample:	9443	9414	9402	1	889
SiO ₂	72.10	67.65	69.19	69.06	70.25
TiO ₂	0.38	0.64	0.49	0.62	0.58
Al ₂ O ₃	13.66	15.28	15.25	15.31	14.56
FeO	2.87	3.94	3.13	4.01	4.14
MnO	0.02	0.06	0.06	0.05	0.06
MgO	0.97	1.46	1.32	1.59	1.24
CaO	1.63	3.12	2.84	2.76	1.89
Na ₂ O	2.71	2.60	2.72	2.75	2.66
K ₂ O	4.05	3.58	3.99	3.76	4.46
P ₂ O ₅	0.14	0.17	0.16	0.18	0.18
	98.53	98.50	99.15	100.09	100.02
Qz	34.16	27.58	28.17		28.47
Co	2.19	1.86	1.66		2.41
Or	23.94	21.16	23.58		28.19
Ab	22.93	22.00	23.01		22.17
An	7.17	14.37	13.09		7.99
Hy	7.10	9.93	8.34		9.32
Il	0.72	1.22	0.93		1.08
Ap	0.33	0.40	0.38		0.45
	98.54	98.52	99.16		100.08
9443	rhyolite ignimbrite, Violet Town Volcanics				
9414	rhyodacite ignimbrite, Violet Town Volcanics				
9402	"schlier" from rhyodacitic ignimbrite, Violet Town Volcanics				
1	calculated VTV parent magma composition				
889	Strathbogie granite, parent composition				

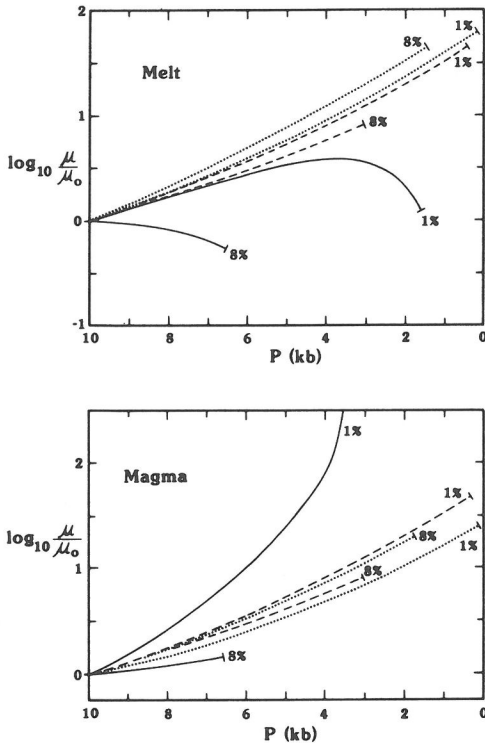


FIG. 11. Variation in viscosity along ascent trajectories as a function of crystallization rate and H₂O content normalized to initial (10 kbar) viscosity value. (a) Melt viscosity. (b) Magma viscosity. Curves designated as in Figure 1. The figures in percent indicate system H₂O content. The intersection with the solidus is indicated by a bar perpendicular to the curve.

stability curve and to the high temperature side of the biotite, plagioclase, and K-feldspar stability curves, as shown in Figure 12 (CLEMENS, 1984, personal communication).

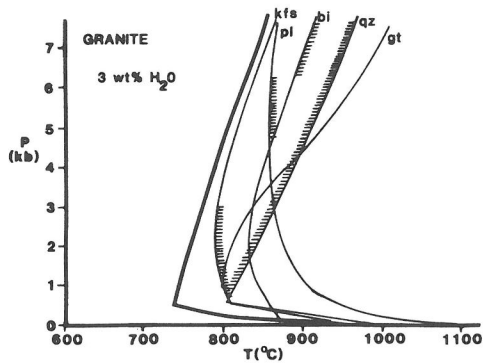


FIG. 12. Simplified experimentally determined phase relationships for the Strathbogie granite with 3 weight percent H₂O in the melt (after CLEMENS, 1981). Hatchures to the right and left of a stability curve indicate that the phase was observed to be present at higher and lower temperature, respectively (CLEMENS, 1984, personal communication). The ascent trajectory must lie within the region bounded by the hatchured curves. See text for discussion.

The Violet Town Volcanics

The Violet Town Volcanics (VTV) consist of approximately 100 km³ of peraluminous intracaldera ignimbrites of late Devonian age (CLEMENS and WALL, 1984). Compositions range from rhyolite to rhyodacite (Table 2) with phenocrysts of quartz + plagioclase + biotite + garnet + cordierite ± hypersthene. Crystal contents range from 0 to 65 modal percent, with biotite forming approximately 20 weight percent, plagioclase 20 to 60 weight percent, and quartz 20 to 40 weight percent of the totals. Crystallization sequence, inferred from textural evidence, was early garnet + quartz, plagioclase and orthopyroxene, followed by biotite, cordierite, and late-stage K-feldspar. CLEMENS and WALL (1984)

Table 3. Model conditions for ascent

Strathbogie Granite	Source	Emplacement
Pressure	5 to 7 kbar	0.5 to 1.0 kbar
T (°C)	>850	>800
Weight percent H ₂ O in Melt	2.8 to 4.0	2.8 to 4.0
Crystal Content	0 to 15%	0 to 50%
Experimental T		
Range at 7 kbar: 3 Weight percent H ₂ O:	905 to 950°C	800 to 817°C
4 Weight percent H ₂ O:	895 to 905°C	745 to 775°C
Violet Town Volcanics	Source	Emplacement
Pressure	3.6 to 6.0 kbar	0.5 to 1.0 kbar
T (°C)	avg. 850	750 to 850
Crystal Content	5%	5%
Experimental T		
Range at 7 kbar: 3 Weight percent H ₂ O:	875 to 900°C	780 to 825°C
4 Weight percent H ₂ O:	825 to 860°C	750 to 780°C

infer early magmatic temperatures of greater than 800 to 830°C and pressures of 3.6 to 6 kbar, with 2.5–4.5 weight percent H₂O. The total restite content is estimated at less than 2 volume percent of easily distinguished garnet, biotite, cordierite, sillimanite, and other phases. Inferred source and emplacement conditions are summarized in Table 3. These results suggest ascent in a largely liquid state and subsequent crystallization in a high level magma chamber. CLEMENS and WALL (1984) infer fluid-absent melting reactions in a source region dominated by weakly to mildly peraluminous quartzo-feldspathic metasedimentary material.

The observed chemical variation in the VTV deposits is interpreted by CLEMENS and WALL (1984) to be a result of about 35% fractional crystallization of parent magma, producing a zoned magma chamber.

Comparison with model ascent trajectories

For comparison of observed and model trajectories, the weight percent H₂O in the melt was first converted to albite-equivalent amount of H₂O, as outlined by BURNHAM (1979), resulting in 3.0 to 4.3 weight percent H₂O in the Strathbogie magma and 3.0 to 4.2 weight percent H₂O in Violet Town Volcanics magma. For purposes of ascent trajectory calculation, the H₂O content of the Strathbogie and VTV magmas are identical; ascent distance and crystal content differ.

Using the conditions given in Table 3, ascent trajectories were calculated for the Strathbogie and Violet Town magmas. Only model ascent trajectories that fit within the maximum and minimum pressure-temperature gradients obtained from Figure 12 were permitted. The 4 weight percent H₂O test case fits well for $P_0 = 7$ kbar for CR = 1.2 to 3.5%/kbar, and at $P_0 = 5$ kbar for CR = 0.3 to 3.5%/kbar. With the minimum H₂O content of 3.0 weight percent, the model trajectories fit from CR = 0 to 3 or 3.5%/kbar at 5 and 7 kbar P_0 . Trajectories for many other H₂O contents and CR's were calculated, but did not fit within the observed minimum and maximum pressure-temperature gradients. The assumed H₂O contents and CR's are held to be correct.

Results for the VTV are similar to those of the Strathbogie, with the exception that crystallization rate is firmly constrained at zero percent. Calculated ascent paths with CR = 0%/kbar fit the experimentally determined ascent regions only for melt H₂O contents of less than about 4 weight percent. The model trajectories fit the experimentally constrained ascent region remarkably well.

Application of model calculations to VTV and Strathbogie magma bodies

The model ascent trajectory which best fits CLEMENS' (1981) results is that for 3 weight percent H₂O, with CR = 0, 5%/kbar initial crystals, initial $P = 5$ to 7 kbar, and initial T about 850°C. For the Strathbogie magmas, crystallization rate is not constrained, so a variety of ascent trajectories can be used to model the system.

By using physical properties calculated for magma along the above ascent trajectories, the possibility of crystal settling and restite segregation in the VTV magma can be examined. Calculations for crystal settling in a convecting magma chamber were performed after MARSH and MAXEY (1985):

$$S = 0.86 \Delta \rho a^2 \left(\frac{g}{\rho \alpha \Delta T L K \mu} \right)^{0.5}, \quad (10)$$

where S is the ratio of crystal settling velocity to convection velocity, K is 10^{-2} cm²/s, L is magma chamber length scale, $\Delta \rho = \rho_{\text{magma}} - \rho_{\text{xl}}$ is magma density, $\alpha = 5 \times 10^{-5}$ deg⁻¹, $g = 980$ cm/s², a = crystal radius, $L = 1$ km, μ = magma viscosity, and $\Delta T = (T_{\text{magma}} - T_{\text{wr}})/2$. Restitic garnet crystals in the VTV have a density of about 3.5 g/cm³ and are about 1 cm in diameter (CLEMENS and WALL, 1984). The T_{wr} is calculated as a function of depth by using:

$$T_{\text{wr}} = T_0 [1 - (z/L)^n], \quad (11)$$

with $n = 2$ and 4 (MARSH, 1982), with $T_0 = 850^\circ\text{C}$ (temperature at initial pressure) and remaining trajectory temperatures lowered accordingly. For $S < 1$, no crystal settling occurs in the magma chamber. By using the above conditions, no crystal settling would occur in a convecting magma chamber for VTV or Strathbogie magmas.

The presence of restite inclusions in the VTV of up to 10 cm diameter also suggests that crystal settling was not an important process during ascent of the magma. By comparing terminal settling velocities for such inclusions with ascent velocities, implies that ascent velocities must have been greater than about 10^{-5} to 10^{-4} cm/s for crystal-magma density contrasts of 0.3 to 0.4 g/cm³. Diapirism was thus probably not the major ascent mechanism for these magmas, because current models for diapiric ascent infer ascent velocities on the order of 10^{-7} to 10^{-5} cm/s (MARSH, 1982).

The relatively high viscosities, particularly at low pressures, imply that the VTV and Strathbogie magmas would be efficient at forcible emplacement and roof lifting. However, Rayleigh numbers calculated for both vertical pipe and horizontal layer

configurations, with $T > 10^3$ degrees, are greater than 10^6 , suggesting that convection would occur for the VTV and Strathbogie magmas both during ascent and after emplacement.

DISCUSSION

Ascent trajectories calculated by using the present model are unique because the ascent trajectory is constrained by the phase equilibria of the magma, rather than the ascent mechanism or physical properties of the magma or wall rocks. The physical properties of the magma (or the magnitudes of their variations) are known along the ascent trajectory as a function of pressure, temperature, and H_2O content of the magma. Specification of crystallization or melting rate does, however, determine the magnitude of heat transfer from the system. To determine whether the rates of heat transfer implied by particular crystallization or melting rates are probable, requires specification of a heat transfer model for a particular ascent mechanism and body geometry. Enthalpy and internal energy data from the present model has been used to constrain ascent velocity and magma body size or shape (SYKES, 1986).

Ascent trajectories

Few other examples exist of pressure-temperature ascent trajectories for magmas of any type. The most common assumption used for pressure-temperature trajectories is that of adiabatic ascent of magma through the crust. Such trajectories are usually calculated using either an expression for the adiabatic gradient,

$$\beta = -g\alpha T/C_p, \quad (12)$$

or adiabatic temperature

$$T = T_0 \exp[\alpha g(z - z_0)/C_p], \quad (13)$$

where α is the coefficient of thermal expansion. Such expressions are strictly applicable only to single phase, single component systems but are often used for magma, assuming average magma property values (Figure 13, curve A). RUMBLE (1976) developed an expression valid for multicomponent, multiphase adiabatic gradients. For the two component system ab- H_2O , with the two phases melt + crystal, RUMBLE'S (1976) adiabats are identical to those determined using the present model (Figure 13, curve B), assuming adiabatic ascent.

Comparison of single phase and multiphase adiabats shows that the gradients in the latter are about 5 times greater than in the former. For example, for 4 weight percent H_2O , the two gradients are 2.5

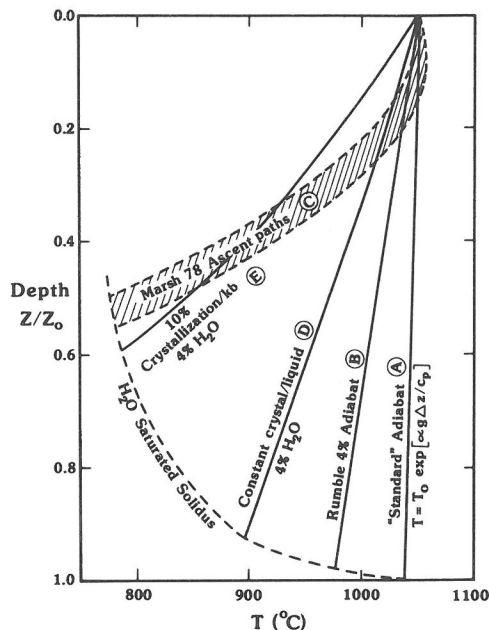


FIG. 13. Comparison of ascent trajectories calculated by using the present model and other models for magma pressure-temperature paths. Dashed line is the H_2O -saturated solidus. A: Standard one-phase adiabat calculated from Equation (13) of text. B: Multiphase adiabat from RUMBLE (1976) for 4 weight percent H_2O in the system. C: General shape of trajectories calculated after MARSH (1978) for diapiric ascent. D: Ascent trajectory, this paper, constant crystal/melt ratio (CR = 0%/kbar). E: Ascent trajectory, this paper, CR = 10%/kbar.

and 0.5 deg/km, respectively. Furthermore, the adiabat calculated in the present model requires fusion of pre-existing crystals (if present) to occur during ascent, at a rate of about 4 to 4.5 weight percent per kbar. This adiabat is not equivalent to an ascent trajectory for MR = 4 to 4.5%/kbar because the melting rate along the adiabat is not linear.

By comparing the model adiabats to model ascent trajectories, temperature gradients for the latter are much greater, on the order of 5 to 14 deg/km for CR = 10%/kbar. The larger value is for low magmatic H_2O contents. Use of adiabatic ascent trajectories in fluid dynamic models of ascent may result in inaccurate temperatures and poor estimates of properties such as viscosity and density, if crystals are initially present in the system. The assumption of adiabatic ascent may be good only for deep-seated diapiric upwelling of partially melting material with high crystal (restite) content, or for melt at superliquidus temperatures.

Non-adiabatic ascent trajectories have been calculated for diapiric ascent of granitic magma using the heat transfer model of MARSH (1978), which

uses the assumption that internal energy change of the ascending magma equals heat transferred away from the body. Calculations were made using a total ascent distance of 30 to 40 km, and $K = 0.01 \text{ cm}^2/\text{s}^2$, with ascent velocities of 10^{-8} to 10^{-4} cm/s and bodies of radius 10^4 to 10^6 cm . Resulting trajectories are shown in Figure 13. The absolute position of trajectories calculated by Marsh's method varies considerably depending on body radius and ascent velocity, but the curvature is nearly constant. It can be seen that the curvature resulting from MARSH's (1978) model is quite distinct from that of the trajectories calculated in the present model (curves D and E). Thus, care must be exercised in using ascent trajectories such as those of MARSH (1978) because they may imply inaccurate assumptions about the physical characteristics of the system. The case Marsh wished to illustrate, CR = 0%/kbar, has a trajectory intermediate to that of the multiphase adiabat and his trajectories. MARSH's trajectories are also sensitive to choice of geotherm and assumptions of initial wall rock and magma temperatures.

Energetics of magma ascent

Most heat transfer models for magma ascent or evolution assume that energy production in an evolving magma body is proportional to $C_p \Delta T$, where ΔT is the temperature difference between the magma and its surroundings, with C_p constant. Energy production within the magma body during ascent is more accurately represented by ΔH or ΔE for the system, as calculated in previous sections. The ΔE includes an amount due to $\Delta(PV)$ work, most often assumed to be zero due to constant system volume. To determine the error resulting from use of $C_p \Delta T$ for magma energy production, effective heat capacities are calculated as $C_p(H) = \Delta H/\Delta T$ and $C(E) = \Delta E/\Delta T$, where ΔH and ΔE are the change in enthalpy and internal energy of the magma system from one (P, T) point to another along the ascent trajectory. The $C_p(H)$ and $C(E)$ are up to three or two times greater than C_p , for CR = 0 to 10%/kbar and 1 to 8 weight percent H_2O . The amount of energy available from a magma body may thus be two to three times greater than that calculated by using $C_p \Delta T$. Results of previous studies of ascent mechanisms where the $C_p \Delta T$ approximation for magma energy is used may, therefore, be in error.

Constancy of magma properties

Fluid dynamic and heat transfer models of evolving or ascending magma bodies often assume

either constant or temperature-dependent magma density, volume, or viscosity. The validity of such assumptions can be evaluated by using data from the present model.

Density is most often assumed to be constant or a function of temperature, such that;

$$\rho = \rho_0 - \rho_0 \alpha (T - T_0), \quad (14)$$

where T_0 and ρ_0 are initial temperature and density, and α is the coefficient of thermal expansion. Numerous theoretical and experimental studies of magma chamber dynamics have demonstrated that compositional variation and crystallization effects on density can dominate the dynamics of a magma chamber (*e.g.*, HUPPERT and SPARKS, 1984). Furthermore, density variations of less than 0.02 g/cm^3 are required for the compositional effects to be important.

In equations estimating velocity of magma ascent or size of magma bodies, the density term is usually to the first power, and variation in magma density is far less than variation in other parameters, so that the assumption of constant ρ_{magma} is not a bad one. From our model calculations, ρ_{magma} is actually constant at CR = 5 to 6%/kbar for 1 to 8 weight percent H_2O , and for other CR's varies by less than 0.015 g/cm^3 per kbar. However, ρ_{melt} can vary from -0.03 to -0.087 g/cm^3 per kbar depending on the H_2O content of the magma and cannot be considered constant.

Equation (14) above yields the temperature dependence of density. By using $\alpha = 5 \times 10^{-5} \text{ deg}^{-1}$, model ascent trajectory temperatures, T , and initial conditions at 10 kbar, calculations yield increasing ρ_{magma} during ascent, whereas when compositional effects are included, ρ_{magma} decreases during ascent for CR < 5 to 6%/kbar. Even at CR = 10%/kbar, Equation (9) yields a value for ρ_{magma} only half that calculated by the present model. These differences are due to the effects of H_2O , pressure, and temperature on density; the former completely dominates temperature and pressure effects.

The effect of crystals on density is also important: $\rho_{\text{magma}} = \rho_{\text{melt}}$ Only for CR = 0%/kbar with no initial crystals. The difference between ρ_{magma} and ρ_{melt} is greatest for systems with large positive crystallization or melting rates. Crystal segregation processes (or other buoyancy-driven processes) will be most effective at low pressures for CR > 0%/kbar and at high pressures for CR < 0%/kbar.

The volume of magma bodies is most often assumed to be constant in fluid dynamic models of magma ascent and evolution. Volume variations calculated for model granite systems show that volume is not constant for ascending magma bodies.

The greatest variation in V_{magma} derives not from ΔV_{xl} but from $\Delta V_{\text{w}}^{\text{m}}$. By assuming constant V_{w}^{m} would result in a 15 to 30% underestimate in total ΔV of the system over an ascent trajectory. By assuming ΔV is due only to crystallization (using 1 bar data), the values for V_{magma} 2 to 4 times too small.

The volume increases predicted by the present model are generally too great to be accommodated by magma bodies or wall rocks. Magma internal pressures can exceed external pressure by 200 bar (an average value for wall rock yield strength) in only 7 to 10 km of ascent for CR = 0%/kbar. Fracturing of wall rocks during ascent in a brittle crust must ensue from such volume increases.

Viscosity of magma and melt plays an important role in internal evolution of magmas during ascent. For examining processes occurring during magma evolution, *e.g.*, crystal settling or convection, variations in viscosity will be important. Three common assumptions used to calculate magma viscosity in previous studies have been (1) μ is constant, (2) μ is a function of temperature only, and (3) use of empirical viscosity relationships. Viscosities calculated by using these assumptions are compared to those calculated using the present model for varying H₂O contents and crystallization rates.

The assumption of constant magma viscosity is good for high crystallization rates and high H₂O contents, because the decrease in viscosity due to increased H₂O is offset by the increase in viscosity due to crystallization. However, at low H₂O contents, a constant value for magma viscosity could be up to four orders of magnitude too low. Melt viscosity can be assumed approximately constant for CR = 10%/kbar and high H₂O contents. The assumption of constant μ_{melt} is worst for CR \leq 0%/kbar and low H₂O contents, yielding a value for viscosity at most 50 times too small.

Viscosity can be assumed to vary as a function of temperature alone, with no contribution by crystals or H₂O content. For low crystallization rates, this is a good assumption, resulting in values for viscosity half those of actual model viscosities. For higher crystallization rates, the assumption that viscosity varies only with temperature results in values for viscosity that differ by up to two orders of magnitude from model viscosities.

SPERA *et al.* (1982) use an empirical relationship for viscosity

$$\mu/\mu_{\infty} = \exp[a(T_{\infty} - T)], \quad (15)$$

where a is a function of H₂O content, crystal content, and composition. The rheological parameter, a , usually varies between 0.02 and 0.10 K⁻¹ (SPERA

et al., 1982). The T is magma temperature, T_{∞} is liquidus temperature, and μ_{∞} is apparent melt viscosity at T . Results from this formulation can be directly compared with model results, because model T 's at P_0 are liquidus temperatures. For CR = 10%/kbar, μ_{m} cannot be duplicated with $a > 0$. For CR = 10%/kbar, μ_{magma} can be approximated by $a \approx 0.02$ for low to intermediate H₂O contents, and by $a \approx 0$ for high H₂O contents. For ascent with CR = 0%/kbar and no initial crystals, $\mu_{\text{magma}} = \mu_{\text{m}}$ and can be approximated by $a \approx 0.02$ for all H₂O contents, by using the temperature from model ascent trajectories.

CONCLUSIONS

The model presented in this paper for calculating ascent trajectories for granitic magmas is consistent with observed petrologic variations, and may be used for calculating P - T - X ascent paths for calc-alkaline, hypersthene- or quartz-normative magmas provided crystallization or melting rate is specified. In addition to ascent trajectories, variation of magma properties, such as volume, energy loss, density, and viscosity, during ascent can be calculated. This information can then be used to test the validity of assumptions made about magma properties, or used directly in model calculations for ascent mechanisms or magma evolution.

Ascent trajectories for MR < about 2%/kbar have positive dP/dT . Adiabatic ascent paths have steeper dP/dT (but are still positive) and require fusion of pre-existing crystals (restite or previously crystallized magma or wall rocks) when present. The usual calculated adiabatic gradient [Equation (12)] is up to 5 times too small for ascending, crystallizing bodies of intermediate H₂O content, because effects of H₂O are ignored.

Water has a large effect on magma properties, especially when crystallization or fusion occur. By neglecting H₂O in granitic magmas, large errors in magma properties can result and physically unrealistic results may be obtained. Melt density and viscosity are important quantities in calculations of crystal separation, crystal settling, or convection; these properties are not constant and cannot be approximated by using standard approaches. Magma density and viscosity can often be correctly assumed constant, or modelled after an empirical relationship such as given in Equation (9). Volume increases in ascending granitic magma bodies for CR < 5 to 6%/kbar, even at low H₂O contents, require expansion of the magma body and concurrent shear deformation of surrounding ductile wall rocks. In the brittle regime, volume increases require the gen-

eration of excess internal magma pressure which will rapidly exceed the strength of wall rocks. Consequent fracturing of wall rocks can lead to partial to complete quench of the magma, or initiation of magma ascent by fracture propagation. Only for CR > 5 to 6%/kbar is the assumption of constant volume consistent with these calculations.

The energetics of ascending granitic magma depends greatly on the contribution of the enthalpy of the hydrous melt component as pressure and degree of crystallization vary, and on the P - V work associated with magma expansion. The energy available from an ascending granitic magma body can reach two to three times that calculated by using heat capacity data. Careful evaluation of ascending magma energetics is necessary for modelling ascent mechanism, ascent distance, and determining the importance of mechanisms such as stoping or wall rock contamination.

Acknowledgments—Financial support for this work was provided by NSF grants EAR8108748-01 and EAR-8407742. This manuscript greatly benefited from comments by Robert W. Luth and an anonymous reviewer. Discussions with John D. Clemens and Alan J. R. White about the ascent model also significantly improved the work.

REFERENCES

- ACKERMANN N. L. and SHEN H. T. (1979) Rheological characteristics of solid-liquid mixtures. *Amer. Inst. Chem. Eng. J.* **25**, 327-332.
- BOETTCHER A. L., BURNHAM C. W., WINDOM K. E. and BOHLEN S. R. (1982) Liquids, glasses and the melting of silicates to high pressures. *J. Geol.* **90**, 127-138.
- BURNHAM C. W. (1979) The importance of volatile constituents. In *The Evolution of the Igneous Rocks*, (ed. H. S. YODER), pp. 439-482 Princeton Univ. Press.
- BURNHAM C. W. (1981) The nature of multicomponent aluminosilicate melts. *Phys. Chem. Earth* **14-15**, 197-229.
- BURNHAM C. W. and DAVIS N. F. (1971) The role of H₂O in silicate melts. I. P - V - T relations in the system NaAlSi₃O₈-H₂O to 10 kilobars and 1000°C. *Amer. J. Sci.* **270**, 54-79.
- BURNHAM C. W. and DAVIS N. F. (1974) The role of H₂O in silicate melts: II. Thermodynamic and phase relations in the system NaAlSi₃O₈-H₂O to 10 kilobars, 700° to 1100°C. *Amer. J. Sci.* **274**, 902-940.
- CHAPPELL B. W. and WHITE A. J. R. (1974) Two contrasting granite types. *Pac. Geol.* **8**, 173-174.
- CLEMENS J. D. (1981) The origin and evolution of some peraluminous acid magmas (experimental, geochemical and petrological investigations). Ph.D. Dissertation, Monash University, Australia.
- CLEMENS J. D. and WALL V. J. (1981) Origin and crystallization of some peraluminous (S-type) granitic magmas. *Can. Mineral.* **19**, 111-131.
- CLEMENS J. D. and WALL V. J. (1984) Origin and evolution of a peraluminous silicic ignimbrite suite: The Violet Town Volcanics. *Contrib. Mineral. Petrol.* **88**, 354-371.
- DINGWELL D. B. (1987) Melt viscosities in the system NaAlSi₃O₈-H₂O-F₂O₋₁. In *Magmatic Processes: Physicochemical Principles*, (ed. B. O. MYSEN), The Geochemical Society Spec. Publ. No. 1, Chap. 00, pp. 000-000.
- HOLLOWAY J. R. (1976) Fluids in the evolution of granitic magmas: Consequences of finite CO₂ solubility. *Bull. Geol. Soc. Amer.* **87**, 1513-1518.
- HUPPERT H. E. and SPARKS R. S. J. (1984) Double-diffusive convection due to crystallization in magmas. *Ann. Rev. Earth Planet. Sci.* **12**, 11-37.
- MARSH B. D. (1978) On the cooling of ascending andesitic magma. *Phil. Trans. Roy. Soc. London* **A288**, 611-625.
- MARSH B. D. (1982) On the mechanics of igneous diapirism, stoping and zone melting. *Amer. J. Sci.* **282**, 808-855.
- MARSH B. D. and KANTHA L. H. (1978) On the heat and mass transfer from an ascending magma. *Earth Planet. Sci. Lett.* **39**, 435-443.
- MARSH B. D. and MAXEY M. R. (1985) On the distribution and separation of crystals in convecting magma. *J. Volcanol. Geotherm. Res.* **24**, 95-150.
- NEKVASIL H. and BURNHAM C. W. (1987) The calculated individual effects of pressure and water content of phase equilibria in the granite system. In *Magmatic Processes: Physicochemical Principles*, (ed. B. O. MYSEN), The Geochemical Society Spec. Publ. No. 1, pp. 433-445.
- RAMBERG H. (1971) Temperature changes associated with adiabatic decompression in geological processes. *Nature* **234**, 539-540.
- READ H. H. (1957) *The Granite Controversy*. T. Murby.
- RUMBLE D. (1976) The adiabatic gradient and adiabatic compressibility. *Carnegie Inst. Wash. Yearb.* **75**, 651-655.
- SHAW H. R. (1972) Viscosities of magmatic silicate liquids: an empirical method of prediction. *Amer. J. Sci.* **272**, 870-893.
- SHAW H. R. (1980) The fracture mechanisms of magma transport from the mantle to the surface. In *Physics of Magmatic Processes*, (ed. R. B. HARGRAVES), pp. 201-264 Princeton Univ. Press.
- SPERA F. J. (1980) Aspects of magma transport. In *Physics of Magmatic Processes*, (ed. R. B. HARGRAVES), pp. 265-323 Princeton Univ. Press.
- SPERA F. J., YUEN D. A. and KIRSCHVINK S. J. (1982) Thermal boundary layer convection in silicic magma chambers: Effects of temperature dependent rheology and implications for thermogravitational chemical fractionation. *J. Geophys. Res.* **87**, 8755-8767.
- SYKES M. L. (1986) Ascent of granitic magma: Constraints from thermodynamics and phase equilibria. Ph.D. Dissertation, Arizona State University.
- TURCOTTE D. L. (1982) Magma migration. *Ann. Rev. Earth Planet. Sci.* **10**, 397-408.
- TURCOTTE D. L. (1987) Physics of magma segregation processes. In *Magmatic Processes: Physicochemical Principles*, (ed. B. O. MYSEN), The Geochemical Society Spec. Publ. No. 1, Chap. 00, pp. 000-000.
- VAN DER MOLEN I. and PATERSON M. S. (1979) Experimental deformation of partially melted granite. *Contrib. Mineral. Petrol.* **70**, 229-318.
- WALDBAUM D. R. (1971) Temperature changes associated with adiabatic decompression in geological processes. *Nature* **232**, 545-547.
- WALTON M. (1955) The emplacement of granite. *Amer. J. Sci.* **253**, 1-18.

